

HIGH-RESOLUTION CONTRAST ENHANCED MULTI-PHASE HEPATIC COMPUTED TOMOGRAPHY DATA FROM A PORCINE RADIO-FREQUENCY ABLATION STUDY

Bernhard Kainz^{1,3}, Philip Voglreiter³, Michael Sereinigg², Iris Wiederstein-Grasser⁶, Ursula Mayrhauser², Sonja Köstenbauer², Mika Pollari⁴, Rostislav Khlebnikov³, Matthias Seise⁹, Tuomas Alhonnoro⁴, Yrjö Häme⁴, Daniel Seider⁵, Ronan Flanagan⁷, Claire Bost⁷, Judith Mühl³, David O'Neill⁸, Tingying Peng⁸, Stephen Payne⁸, Daniel Rueckert¹, Dieter Schmalstieg³, Michael Moche⁵, Marina Kolesnik⁹, Philipp Stiegler², and Rupert H. Portugaller¹⁰

¹ Department of Computing, Imperial College London, UK

² Department for Surgery, Division for Transplant Surgery Medical University Graz, AUT

³ Institute for Computer Graphics and Vision (ICG), Graz University of Technology, AUT

⁴ Department of Biomedical Engineering and Computational Science, Aalto University, FI

⁵ Department of Diagnostic and Interventional Radiology, Leipzig University Hospital, Leipzig, GER

⁶ Division of Biomedical Research and Section for Surgical Research, Medical University Graz, AUT

⁷ NUMA Engineering Services Ltd., Dundalk, Co. Louth, IRE

⁸ Department of Engineering Science, Keble College, Oxford, UK

⁹ Fraunhofer Institute for Applied Information Technology, Schloss Birlinghoven, GER

¹⁰ University Clinic of Radiology, Medical University Graz, AUT

ABSTRACT

Data below 1 mm voxel size is getting more and more common in the clinical practice but it is still hard to obtain a consistent collection of such datasets for medical image processing research. With this paper we provide a large collection of Contrast Enhanced (CE) Computed Tomography (CT) data from porcine animal experiments and describe their acquisition procedure and peculiarities. We have acquired three CE-CT phases at the highest available scanner resolution of 57 porcine livers during induced respiratory arrest. These phases capture contrast enhanced hepatic arteries, portal venous veins and hepatic veins. Therefore, we provide scan data that allows for a highly accurate reconstruction of hepatic vessel trees. Several datasets have been acquired during *Radio-Frequency Ablation* (RFA) experiments. Hence, many datasets show also artificially induced hepatic lesions, which can be used for the evaluation of structure detection methods.

Index Terms— contrast enhanced computed tomography, liver tumor ablation, porcine study data

1. INTRODUCTION

Contrast Enhanced (CE) Computed Tomography (CT) is a valuable tool to analyze vascular structures within the body.

Arteries and veins, which would be invisible without contrast agent, show clearly as bright structures after injecting an X-Ray absorbing iodine-based agent. The contrast agent is usually administered intravenously and is transported through the body without significant dissipation for a certain time. This area of concentrated contrast agent in the blood can be observed moving through the body and is usually called contrast agent *bolus*. A *bolus* is first transported to the heart, from where it enters the arterial vessel system. From the arteries the contrast agent perfuses through the body's tissues to the veins, which transport it back to the heart. Consecutive scans, correctly timed after the injection, will therefore show first bright arteries and then bright veins. The timing of the scans is crucial for this imaging sequence because the *bolus* will only be concentrated for a short period of time and the contrast agent will distribute evenly through the body shortly after the injection. This even distribution raises the average image intensity and, along with the risk of contrast agent intoxication, limits the number of times a CE scan can be performed for a single patient.

Usually, the CE scan sequence is triggered automatically by placing a region of interest (ROI) into a continuously scanned slice through the subject's aorta. Previously calculated delays and amount of contrast agent – depending on the targeted organ and the subject's body mass – are applied and the scan sequence is started as soon as the image intensity reaches a certain threshold in the ROI. Targeting the liver for CE-CT forms a special case. The liver contains the *hepatic arterial*

*This work is supported by the European Community's FP7 under grant agreement no. 223877 (IMPPACT), and 600641 (Go-Smart), coordinated by Marina Kolesnik. Bernhard Kainz is supported by a Marie Curie Intra-European Fellowship (FP7-PEOPLE-2012-IEF F.A.U.S.T. 325661).

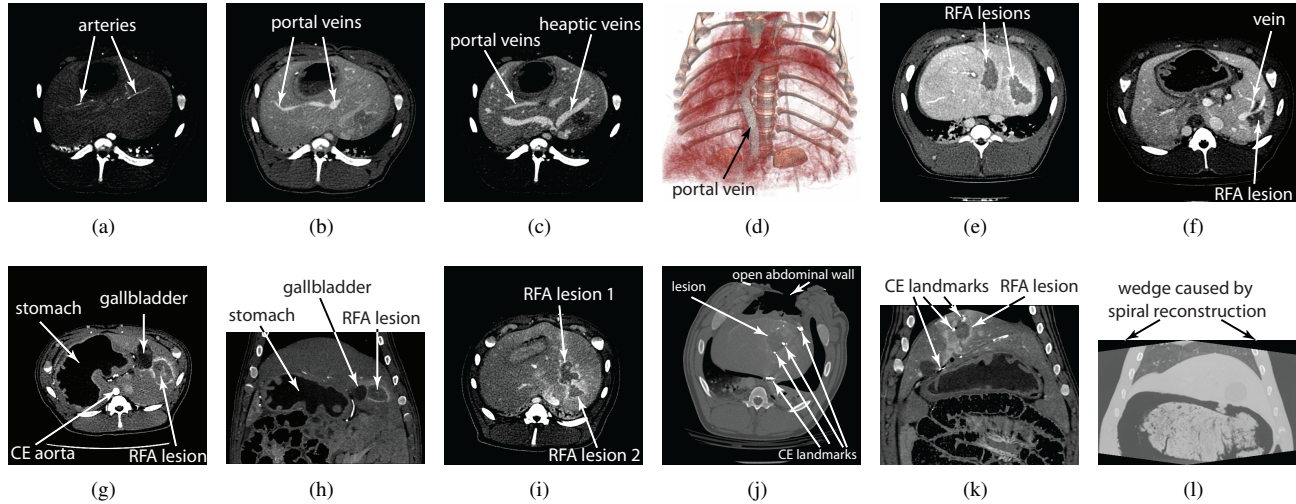


Fig. 1. Overview over the datasets. The window-level is adjusted in all images to highlight the discussed features. (a)–(d) show the target sequence on the example of Pig 36: contrast enhanced arteries (a), contrast enhanced portal veins (b), contrast enhanced hepatic veins (c), and an overview over this dataset in 3D (d). (e)–(h) show artificially induced RFA lesions for Pig 18 (e), 19 (f), and 34 (g) axial and coronal for Pig 34 (h). Note that RFA lesions must not be mistaken with the pig’s gallbladder, marked in (g) and (h). (i)–(l) show selected specialties of our datasets. RFA lesions may grow together if they have been induced too close to each other (i) (Pig 43); some experiments took place with an open abdomen of the pig and artificially injected *landmarks* (a mixture of tissue glue and CT contrast agent) (j) axial and (k) coronal (Pig 53). Whenever it was possible we tried to acquire a whole volume within one rotation of the 320 rows CT detector. This reduces motion artifacts and provides a high resolution but the reconstruction is not completely cubic anymore. The borders of this *spiral* reconstruction are filled with the lowest possible intensity values in the image. (l) shows this effect on the example of Pig 14.

vessel tree, the *hepatic venous vessel tree*, and a *hepatic portal venous vessel tree*. The portal venous vessel tree conducts blood from the gastrointestinal tract and spleen to the liver and will show a higher contrast agent saturation shortly before the hepatic veins are enriched. We make use of this fact and perform three scans after the injection of a contrast agent bolus in a series of animal experiments. Even though exact separation of the portal and hepatic veins is not possible, the two venous scans show different contrast levels for the two vessel trees. This differs from clinical practice where only two scans are performed after bolus injection. The animal experiments have been performed in the course of the project *IMPACT*, with the goal to develop a patient-specific intervention planning and monitoring application for Radiofrequency Ablation (RFA) of malignant liver tumours. RFA is a minimally invasive form of cancer treatment, which is achieved by placing a needle inside the malignancy and destroying it through intensive heating. Because vessels form a heat-sink [1] during this procedure, which may allow malicious cancer cells to survive, highly accurate imaging of the hepatic vessels has been necessary. Therefore, besides the vessel trees, most of our scans also show two artificially induced RFA lesions, which are noticeable by a lower contrast agent saturation.

Related Work: Publicly available hepatic CT dataset are rare and provide either only a few high-resolution or multi-

model scans [2, 3] or target different organs. The most comprehensive publicly available hepatic CT database, which we are aware of, consists of 10 patient scans [4] and was performed within the acceptable dose and contrast agent limits for human patients. Because we are providing animal experiment data, we can use a higher dose of contrast agent than usually allowed in patients. Therefore, our datasets have a uniquely high contrast and resolution. Furthermore, patients suffering from hepatocellular carcinoma often show a lower perfusion in the liver, which lowers the image quality in contrast to our mostly healthy pigs.

Our scans are performed in a similar way as proposed by [5], who presented a way for the correct bolus timing to acquire data from all three hepatic vessel trees separately.

2. IMAGE ACQUISITION

All authorized animal experiments, including medication, anaesthesia and euthanasia, have been carried out according to the Austrian animal law. The pigs have been anaesthetized by a professional veterinarian using Remifentanyl (Ultivar, GlaxoSmithKline Pharma GmbH, Vienna, Austria) 1 mg ad. 50 ml NaCl 0.9% (20 g/ml) 0.08–0.1 g/kg/KG/h and Sevourane (SEVOfluranr, Abbott Laboratories, Illinois, US) 2% ET. CT scans were performed using a 320 rows Aquilion One CT System, Toshiba Medical Systems, (Austria) using

Pig	CA [ml]	art [s]	pv [s]	hv [s]	DENA [days]	RFA ls.	RFA probe	voxel size x,y,z [mm]	max dim x,y,z [voxels]	comments
1	40	5	8	15	–	1	RITA	0.60,0.60,0.50	512,512,320	hv delay too short
2	40	5	15	25	–	2	RITA	0.51,0.51,0.50	512,512,320	–
3	40	5	10	20	–	2	RITA	0.46,0.46,0.50	512,512,320	pv delay too short
4	40	5	15	20	–	2	RITA	0.35,0.35,0.50	512,512,320	–
5	30	5	15	20	–	2	RITA	0.37,0.37,0.50	512,512,320	–
6	30	5	15	20	–	2	RITA	0.38,0.38,0.50	512,512,320	–
7	30	5	15	20	–	2	RITA	0.41,0.41,0.50	512,512,320	–
8	40	5	15	20	–	2	Radionics	0.49,0.49,0.50	512,512,320	–
9	40	5	15	20	–	2	Radionics	0.54,0.54,0.50	512,512,320	–
10	40	5	15	20	35	–	–	0.63,0.63,0.30	512,512,734	–
11	40	5	15	20	35	–	–	0.63,0.63,0.30	512,512,684	hv delay too long
12	80	5	13	50	307	–	–	0.63,0.63,0.30	512,512,901	~115 kg weight
13	60	5	8	15	52	–	–	0.63,0.63,0.30	512,512,851	pv, hv delay too short
14	40	5	8	15	–	1	RITA	0.50,0.50,0.50	512,512,320	–
15	40	5	8	15	–	2	RITA	0.50,0.50,0.50	512,512,320	–
16	40	5	8	15	–	2	Radionics	0.50,0.50,0.50	512,512,320	low hv contrast
17	40	5	8	15	–	2	Radionics	0.50,0.50,0.50	512,512,320	–
18	40	5	8	15	–	2	RITA	0.45,0.45,0.50	512,512,320	–
19	40	5	8	15	–	2	RITA	0.46,0.46,0.50	512,512,320	1 lesion between lobes (small)
20	40	5	8	15	–	2	RITA	0.45,0.45,0.50	512,512,320	–
21	40	5	8	15	–	2	RITA	0.45,0.45,0.50	512,512,320	low contrast lesions
22	100	5	10	50	258	–	–	0.51,0.51,0.30	512,512,531	low hv contrast, ~150 kg weight
23	100	5	8	15	271	–	–	0.67,0.67,0.50	512,512,791	~150 kg weight, inflated stomach
24	100	5	8	15	271	–	–	0.50,0.50,0.50	512,512,320	~150 kg weight
25	40	5	8	15	47	–	–	0.50,0.50,0.50	512,512,320	died w/o RFA
26	40	5	15	30	–	2	RITA	0.50,0.50,0.50	512,512,320	–
27	40	5	15	35	–	2	RITA	0.50,0.50,0.50	512,512,320	–
28	40	5	8	15	–	–	–	0.63,0.63,0.30	512,512,601	moved during scan, low hv contrast
30	40	5	15	50	–	2	RITA	0.50,0.50,0.50	512,512,320	–
31	40	5	15	50	–	2	RITA	0.50,0.50,0.50	512,512,320	–
34	40	5	15	50	–	2	RITA	0.63,0.63,0.30	512,512,634	–
35	40	5	15	50	–	2	RITA	0.51,0.51,0.30	512,512,607	–
36	40	5	13	35	–	2	RITA	0.51,0.51,0.30	512,512,674	–
37	40	5	13	25	–	2	RITA	0.52,0.52,0.30	512,512,681	–
38	40	5	15	25	–	2	RITA	0.51,0.51,0.30	512,512,581	–
39	40	5	15	25	–	2	RITA	0.51,0.51,0.30	512,512,561	–
40	40	5	15	25	–	2	RITA	0.47,0.47,0.30	512,512,754	–
41	40	5	15	25	–	2	RITA	0.54,0.54,0.30	512,512,754	–
42	40	5	15	25	–	2	RITA	0.51,0.51,0.30	512,512,647	–
43	40	5	15	25	–	2	RITA	0.54,0.54,0.30	512,512,607	–
44	100	5	15	25	272	–	–	0.71,0.71,0.30	512,512,867	low pv, hv contrast, ~150 kg weight
45	40	5	15	25	–	2	RITA	0.63,0.63,0.30	512,512,594	–
46	40	5	15	25	–	2	RITA	0.63,0.63,0.30	512,512,587	–
47	110	5	15	25	309	–	–	0.66,0.66,0.30	512,512,681	low pv, hv contrast, ~180 kg weight
48	110	5	15	25	355	–	–	0.63,0.63,0.30	512,512,614	~180 kg weight
53	40	5	15	25	–	1	RITA	0.53,0.53,0.30	512,512,694	open abdomen with CE landmarks
56	40	5	15	25	239	–	–	0.70,0.70,0.30	512,512,914	low hv contrast
57	40	5	15	25	146	–	–	0.72,0.72,0.30	512,512,1007	low hv contrast, died w/o RFA
58	40	5	15	25	–	1	RITA	0.63,0.63,0.30	512,512,607	open abdomen with CE landmarks
59	40	5	15	25	–	1	RITA	0.57,0.57,0.30	512,512,757	open abdomen, low hv contrast
60	40	5	15	25	158	2	RITA	0.50,0.50,0.30	512,512,607	high DENA dose
61	40	5	15	25	138	1	RITA	0.69,0.69,0.30	512,512,821	high DENA dose, CE landmarks, low hv
62	40	5	15	25	291	2	RITA	0.67,0.67,0.30	512,512,867	high DENA dose
63	40	5	15	25	120	–	–	0.70,0.70,0.30	512,512,821	high DENA dose, low hv contrast
64	40	5	15	25	242	2	RITA	0.69,0.69,0.30	512,512,947	high DENA dose, low hv contrast
97	40	5	15	50	–	–	–	0.63,0.63,0.30	512,512,634	low hv contrast
98	40	5	15	50	–	–	–	0.63,0.63,0.30	512,512,651	–

Table 1. Summary of the available datasets. We use our own experiment IDs as identifier of the datasets (*Pig*) to keep consistency with our database. These IDs are also used as name scheme in the downloadable datasets. In this table we also give information on the amount of used contrast agent (*CA*), which mainly depends on the animal’s weight, the used scan delay for the arterial (*art*), portal-venous (*pv*) and hepatic-venous (*hv*) CE scans, the time of the exposure to DENA (*DENA*), the number of RFA lesions (*RFA ls.*) and the used RFA probe, together with the dimensions of the datasets and further comments for special cases. The weight of the animals has been between 35 and 55 kg, unless otherwise stated.

120kV, 250mAs, a *body standard FC 17* reconstruction filter, and a helical pitch of 53. For the scan and during anaesthesia the pig has been artificially ventilated and placed in a plastic laundry basket to stabilize its position.

For RFA research, a radiologist inserted an RFA probe (**RITA** StarBurstr XL, Electrosurgical Device, RITA Medical System, CA, US or **Radionics** Cool-tip, Covidien Surgical Solutions Group, CO, US) into the liver during respiratory arrest under image guidance and induced a 3–5 cm large lesion. This procedure has been repeated once in most of the cases to get two separate lesions at previously defined positions. At the end of the procedure, a 3-phase CE-CT scan was performed using 40–110 ml contrast agent under artificial respiratory arrest. The three contrast phases have been acquired after placing a ROI into the pig’s continuously scanned aorta. As soon as the image intensity exceeded a predefined threshold, the image sequence has been triggered according to the delays given in Table 1. We have configured the scanner to acquire images at the highest available resolution for the given field of view. The scan volume has been adjusted by a radiographer to cover the whole liver. Depending on the animal’s size, the scan volume can either fit within the 160 mm detector array of the scanner, which allows to reconstruct a whole $512 \times 512 \times 320$ voxels volume per rotation with 0.5mm slice distance after one 0.5s rotation of the detector array (*spiral reconstruction*), or, for larger scan areas, several rotations with $0.5mm \times 64slices$ have been used internally by the scanner to reconstruct a larger volume with a lower slice distance of 0.3mm. The in-plane resolution depends also on the chosen scan volume and has been adjusted to be as high as possible. The feed-head direction of the animal in the scanner has been chosen depending on the planned experiment, i.e., some scans can appear upside down. We have also tried to induce cirrhosis and hepatocellular carcinomas by injections of N-Nitrosodiethylamine (**DENA**) once a week. That means that some of our scan data show different levels of cirrhosis and therefore different perfusion levels. The time of *DENA* exposure is also summarized in Table 1.

3. APPLICATIONS

The datasets are available online¹ and Figure 1 shows selected annotated slices of the resulting scans. The data has been used for various applications. In [6] we could show that our datasets allow for vessel segmentation with an error less than one voxel. [7, 8] discuss how to use these datasets for access path decision support for minimal invasive interventions and [9] use the segmentation results from these datasets to build a model for RFA ablations, which is able to accurately predict the cooling effect of vessels during the RFA procedure.

The datasets are collected in separate *rar*-compressed archives. Each archive contains three contrast phases per pig. The files are saved in *nifti* format [10] for the widest possible com-

patibility. The original scan resolution and orientation are contained in the header section of each *nii*-file.

4. CONCLUSIONS

We have presented a database of 57 high resolution hepatic CE-CT scans from a porcine RFA study. These datasets can be freely used for research in medical image processing and visualization and allows evaluation of these algorithms for image quality that is not yet available for human patients.

We believe that our datasets will help to develop novel techniques and that as much value as possible can be gained from the scarification of the animals. In future we plan to amend the data with expert segmentations of the liver.

5. REFERENCES

- [1] D.S.K. Lu, S.S. Raman, D.J. Vodopich, M. Wang, J. Sayre, and C. Lassman, “Effect of vessel size on creation of hepatic radiofrequency lesions in pigs,” *Am J Roentgenology*, vol. 178, no. 1, pp. 47–51, 2002.
- [2] V. Vesna, “The visible human project: Informatic bodies and posthuman medicine.,” *AI Soc.*, vol. 14, no. 2, pp. 262–263, 2000.
- [3] OsiriX, “Dicom sample image sets,” website, July 2013.
- [4] B.J. Erickson, “TCGA-LIHC,” Mayo Clinic, Rochester, MN, July 2013.
- [5] W. Dennis Foley, Thomas A. Mallisee, Mark D. Hohenwarter, Charles R. Wilson, Francisco A. Quiroz, and Andrew J. Taylor, “Multiphase Hepatic CT with a Multirow Detector CT Scanner,” *Am J Roentgenology*, vol. 175, no. 3, pp. 679–685, 2000.
- [6] T. Alhonnoro, M. Pollari, M. Lilja, R. Flanagan, B. Kainz, J. Muehl, U. Mayrhauser, R.H. Portugaller, P. Stiegler, and K. Tscheliessnigg, “Vessel segmentation for ablation treatment planning and simulation,” in *Proc. MICCAI’10*, 2010, pp. 45–52.
- [7] B. Kainz, M. Grabner, A. Bornik, S. Hauswiesner, J. Muehl, and D. Schmalstieg, “Ray casting of multiple volumetric datasets with polyhedral boundaries on manycore GPUs,” *ACM Trans. Graph.*, vol. 28, no. 5, pp. 152:1–152:9, Dec. 2009.
- [8] R. Khlebnikov, B. Kainz, J. Muehl, and D. Schmalstieg, “Crepuscular rays for tumor accessibility planning,” *IEEE TVCG*, vol. 17, no. 12, pp. 2163–2172, Dec. 2011.
- [9] S. Payne, R. Flanagan, M. Pollari, T. Alhonnoro, C. Bost, D. O’Neill, T. Peng, and P. Stiegler, “Image-based multi-scale modelling and validation of radiofrequency ablation in liver tumours,” *Phil. Trans. R. Soc. A. Mathematical Physical and Engineering Sciences*, vol. 11, pp. 4233–5, 2011.
- [10] B. Whitcher, V.J. Schmid, and A. Thornton, “Working with the DICOM and NIFTI data standards in R,” *Journal of Statistical Software*, vol. 44, no. 6, pp. 1–28, 2011.

¹<http://www.gosmart-project.eu/datasets.php>